An efficient kinetic modeling in plasmas by using the AWBS transport equation

M. Holec*

Centre Lasers Intenses et Applications,
Universite de Bordeaux-CNRS-CEA,
UMR 5107, F-33405 Talence, France.

J. Nikl

ELI-Beamlines Institute of Physics, AS CR, v.v.i,
Na Slovance 2, Praha 8, 180 00, Czech Republic and
Czech Technical University in Prague, Faculty of Nuclear Sciences and
Physical Engineering, Brehova 7, 115 19 - Praha 1, Czech Republic.

S. Weber

ELI-Beamlines Institute of Physics, AS CR, v.v.i,
Na Slovance 2, Praha 8, 180 00, Czech Republic.

(Dated: June 25, 2018)

Text of abstract.

I. INTRODUCTION

A more generally valid approach to the problem of treating changes in a distribution function resulting each of which from frequently occurring "events", produces a small change in the momentum of a particle, is to use the Fokker-Planck equation [1], which has been discussed by Spitzer and collaborators [2, 3] . They used the formalism of this equation to evaluate the collision terms of the Boltzmann equation under the assumptions that (a) the events producing changes in particle momenta are two-body interactions described by the associated differential scattering cross sections, and (b) that the distribution function is of the form $f^0 + \mu f^1$, where f^0 and f^1 are isotropic and μ, is the direction cosine between the particle trajectory and some preferred direction in space, and is assumed to be small.

It is the purpose of this paper to present the mechanics of two-body collisions in a somewhat simplified form, and to derive the Fokker-Planck equation for an function. From this general arbitrary distribution equation such special cases as those of Chandrasekhar and Spitzer may easily be obtained. For more complex situations the equation is suitable for integration by an electronic computer [4].

AWBS [5]

II. THE AWBS KINETIC MODEL

$$\frac{\partial f}{\partial t} + \boldsymbol{v} \cdot \nabla_{\boldsymbol{x}} f + \tilde{\boldsymbol{E}} \cdot \nabla_{\boldsymbol{v}} f = C_{ee}(f) + C_{ei}(f),$$

$$C_{FP}(f) = \Gamma \int \nabla_{\boldsymbol{v}} \nabla_{\boldsymbol{v}} (\boldsymbol{v} - \tilde{\boldsymbol{v}}) \cdot (f \, \nabla_{\tilde{\boldsymbol{v}}} f - f \, \nabla_{\boldsymbol{v}} f) \, \mathrm{d}\tilde{\boldsymbol{v}},$$

where $\Gamma = \frac{q_e^4 \ln\Lambda}{4\pi\epsilon^2 m_e^2}$.

Fish high-velocity limit collision operator [6] AWBS [5] Sorbo [7, 8]

$$C_H = v\nu_e \frac{\partial}{\partial v}\left(f + \frac{v_{th}^2}{v}\frac{\partial f}{\partial v}\right)$$
$$+ \frac{\nu_e}{2}\left(1 - \frac{v_{th}^2}{2v^2}\right)\left(\frac{\partial}{\partial \mu}\left((1-\mu^2)\frac{\partial f}{\partial \mu}\right) + \frac{1}{\sin^2(\phi)}\frac{\partial^2 f}{\partial \theta^2}\right), \tag{1}$$

The Maxwell-Boltzmann averaged e-e scattering in (1) can be approximated as $\nu_e \int \left(1 - \frac{v_{th}^2}{2v^2}\right) f_M 4\pi v^2 \,\mathrm{d}v = \frac{\nu_e}{2}$.

A simplified kinetic formulation to the Fokker-Planck collision operator for electrons combining [6] and [5] was introduced in [7].

$$C_{AWBS} = v\frac{\nu_e}{2}\frac{\partial}{\partial v}\left(f - f_M\right)$$
$$+ \frac{\nu_{ei} + \frac{\nu_e}{2}}{2}\left(\frac{\partial}{\partial \mu}\left((1-\mu^2)\frac{\partial f}{\partial \mu}\right) + \frac{1}{\sin^2(\phi)}\frac{\partial^2 f}{\partial \theta^2}\right), \tag{2}$$

III. BGK, AWBS, AND FOKKER-PLANCK MODELS IN LOCAL DIFFUSIVE REGIME

We can try to find an approximate solution while using the first term of expansion in λ_{ei} and μ as

$$\tilde{f}(z, v, \mu) = f^0(z, v) + f^1(z, v)\lambda_{ei}\mu, \tag{3}$$

where $\lambda_{ei} = \frac{v}{\nu_{ei}} = \frac{v^4}{Z n_e \Gamma}$.

* milan.holec@u-bordeaux.fr

$$\mu\left(\frac{\partial\tilde{f}}{\partial z}+\frac{\tilde{E}_z}{v}\frac{\partial\tilde{f}}{\partial v}\right)+\frac{\tilde{E}_z(1-\mu^2)}{v^2}\frac{\partial\tilde{f}}{\partial\mu}= \mu\left(\frac{\partial f^0}{\partial z}+\frac{\tilde{E}_z}{v}\frac{\partial f^0}{\partial v}\right)+\frac{\tilde{E}_z\lambda_{ei}}{v^2}f^1+O(\mu^2),$$

A. The BGK local diffusive electron transport

$$\frac{1}{v}C_{BGK}(f)=\frac{f-f_M}{\lambda_e}+\frac{1}{2\lambda_{ei}}\frac{\partial}{\partial\mu}(1-\mu^2)\frac{\partial f}{\partial\mu}, \tag{4}$$

$$f^0=f_M+\frac{\tilde{E}_z}{v^2}f^1 Z\lambda_{ei}^2, \tag{5}$$

$$f^1=-\frac{Z}{Z+1}\left(\frac{\partial f^0}{\partial z}+\frac{\tilde{E}_z}{v}\frac{\partial f^0}{\partial v}\right), \tag{6}$$

and when holds

$$\boldsymbol{j}\equiv q_e\int\boldsymbol{v}f^1\,\mathrm{d}\boldsymbol{v}=\boldsymbol{0}\rightarrow\tilde{\boldsymbol{E}}=v_{th}^2\left(\frac{\nabla\rho}{\rho}+\frac{5}{2}\frac{\nabla T}{T}\right),$$

i.e. the electric field $\tilde{E}_z$ obeying the zero current condition leads to

$$\tilde{f}=f_M-\frac{Z}{Z+1}\left(\frac{v^2}{2v_{th}^2}-4\right)\frac{1}{T}\frac{\partial T}{\partial z}f_M\lambda_{ei}\mu,$$

B. The AWBS diffusive electron transport

$$\frac{1}{v}C_{AWBS}(f)=\frac{v}{2\lambda_e}\frac{\partial}{\partial v}\left(f-f_M\right)+\frac{1}{2}\left(\frac{1}{\lambda_{ei}}+\frac{1}{2\lambda_e}\right)\frac{\partial}{\partial\mu}(1-\mu^2)\frac{\partial f}{\partial\mu}, \tag{7}$$

$$\frac{\partial}{\partial v}\left(f^0-f_M\right)=\frac{\tilde{E}_z}{v^3}f^1 2Z\lambda_{ei}^2, \tag{8}$$

$$\frac{v}{2Z\lambda_{ei}}\frac{\partial\left(f^1\lambda_{ei}\right)}{\partial v}-\frac{2Z+1}{2Z}f^1=\frac{\partial f^0}{\partial z}+\frac{\tilde{E}_z}{v}\frac{\partial f^0}{\partial v}$$

$$\frac{\partial f^1}{\partial v}+\frac{1}{v}(3-2Z)f^1= \frac{2Z}{v}\left(\frac{1}{\rho}\frac{\partial\rho}{\partial z}+\left(\frac{v^2}{2v_{th}^2}-\frac{3}{2}\right)\frac{1}{T}\frac{\partial T}{\partial z}-\frac{\tilde{E}_z}{v_{th}^2}\right)f_M. \tag{9}$$

C. The Fokker-Planck diffusive electron transport

The Fokker-Plank collision operator can be written as [9]

$$\frac{1}{v}C_{FP}(f)=\frac{\Gamma}{v}\left(4\pi f^2+\frac{\nabla_{\boldsymbol{v}}\nabla_{\boldsymbol{v}}f:\nabla_{\boldsymbol{v}}\nabla_{\boldsymbol{v}}g}{2}\right),$$

where $g(\boldsymbol{v})=\int|\boldsymbol{v}-\tilde{\boldsymbol{v}}|f(\tilde{\boldsymbol{v}})\,\mathrm{d}\tilde{\boldsymbol{v}}$ is the Rosenbluth potential [4]. Since we are interested in the approximate solution in the diffusive regime, it is convenient to use a low anisotropy approximation $\tilde{g}=g^0(f^0)+g^1(f^1)\lambda_{ei}\mu$, which arises from Eq. 45 in [4].

$$\begin{aligned}C_{FP}(\tilde{f})=\Gamma&\left(4\pi {f^0}^2+\frac{1}{2}\frac{\partial^2 f^0}{\partial v^2}\frac{\partial^2 g^0}{\partial v^2}+\frac{1}{v^2}\frac{\partial f^0}{\partial v}\frac{\partial g^0}{\partial v}\right)\\
&+\frac{\mu}{Zn_e}\Bigg[8\pi f^0 f^1 v^4-v\left(\frac{\partial f^0}{\partial v}g^1+\frac{\partial g^0}{\partial v}f^1\right)\\
&+\frac{1}{v^2}\left(\frac{\partial f^0}{\partial v}\frac{\partial(g^1v^4)}{\partial v}+\frac{\partial g^0}{\partial v}\frac{\partial(f^1v^4)}{\partial v}\right)\\
&+\frac{1}{2}\left(\frac{\partial^2 f^0}{\partial v^2}\frac{\partial^2(g^1v^4)}{\partial v^2}+\frac{\partial^2 g^0}{\partial v^2}\frac{\partial^2(f^1v^4)}{\partial v^2}\right)\Bigg]+O(\lambda_{ei}^2,\mu^2),\end{aligned}$$

where the isotropic contribution $O(\lambda_{ei}^2)=\frac{2}{v^2}\left(\frac{\partial f^1\lambda_{ei}}{\partial v}-\frac{f^1\lambda_{ei}}{v}\right)\left(\frac{\partial g^1\lambda_{ei}}{\partial v}-\frac{g^1\lambda_{ei}}{v}\right)$.

$$\begin{aligned}4\pi {f^0}^2+\frac{1}{2}\frac{\partial^2 f^0}{\partial v^2}\frac{\partial^2 g^0}{\partial v^2}+\frac{1}{v^2}\frac{\partial f^0}{\partial v}\frac{\partial g^0}{\partial v}=\frac{\tilde{E}_z}{v^5}f^1 Zn_e\lambda_{ei}^2\\
-\frac{2}{v^2}\left(\frac{\partial f^1\lambda_{ei}}{\partial v}-\frac{f^1\lambda_{ei}}{v}\right)\left(\frac{\partial g^1\lambda_{ei}}{\partial v}-\frac{g^1\lambda_{ei}}{v}\right),\end{aligned} \tag{10}$$

where the fundamental property of the Fokker-Planck collision operator is to tend to Maxwell-Boltzmann distribution [10], i.e. $f^0=f_M$.

$$\begin{aligned}\frac{1}{Zn_e}\Bigg[\frac{1}{2}\left(\frac{\partial^2 f_M}{\partial v^2}\frac{\partial^2(g^1v^4)}{\partial v^2}+\frac{\partial^2 g_M}{\partial v^2}\frac{\partial^2(f^1v^4)}{\partial v^2}\right)\\
+\frac{1}{v^2}\left(\frac{\partial f_M}{\partial v}\frac{\partial(g^1v^4)}{\partial v}+\frac{\partial g_M}{\partial v}\frac{\partial(f^1v^4)}{\partial v}\right)\\
-v\left(\frac{\partial f_M}{\partial v}g^1+\frac{\partial g_M}{\partial v}f^1\right)+8\pi f_M f^1 v^4\Bigg]-vf^1\\
=v\frac{\partial f_M}{\partial z}+\tilde{E}_z\frac{\partial f_M}{\partial v},\end{aligned} \tag{11}$$

$$f_1(v,\mu)=\mu\frac{m_e^2}{4\pi e^4\ln\Lambda}\frac{v_{2th}^4}{Z}\left(2d_T(v/v_{2th})+\frac{3}{2}\frac{\gamma_T}{\gamma_E}d_E(v/v_{2th})\right)\frac{f_M(v)}{n_e}\frac{\nabla T}{T}, \tag{12}$$

where $d_T(x)=ZD_T(x)/B$ and $d_E(x)=ZD_E(x)/A$ are represented by numerical values in TABLE I and TABLE II in [3], respectively.

	$Z=1$	$Z=2$	$Z=4$	$Z=16$	$Z=116$
$\bar{\Delta}\boldsymbol{q}_{AWBS}$	0.057	0.004	0.038	0.049	0.004

TABLE I. Relative error $\bar{\Delta}\boldsymbol{q}_{AWBS} = |\boldsymbol{q}_{AWBS} - \boldsymbol{q}_{SH}|/\boldsymbol{q}_{SH}$ of the AWBS kinetic model equation (2) showing the discrepancy (maximum around 5%) with respect to the original solution of the heat flux given by numerical solution in Spitzer and Harm [3].

D. Summary of BGK, AWBS, and Fokker-Planck diffusion

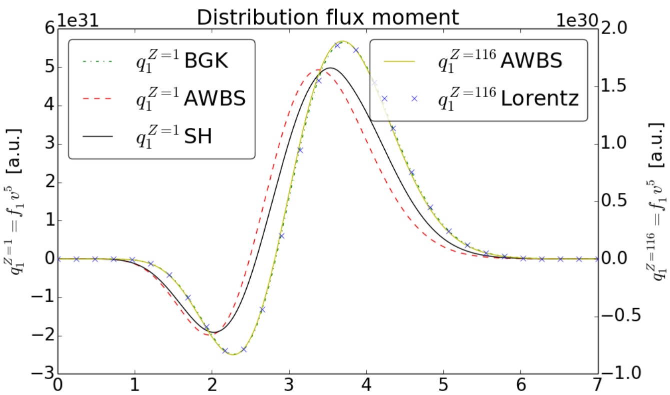

FIG. 1. The flux velocity moment of the anisotropic part of the electron distribution function in low $Z = 1$ and high $Z = 116$ plasmas in diffusive regime.

IV. BENCHMARKING THE AWBS NONLOCAL TRANSPORT MODEL

A. AP1 implementation

In order to eliminate the dimensions of the above transport problem the first-two-moment model based on approximation

$$\tilde{f} = \frac{f_0}{4\pi} + \frac{3}{4\pi}\boldsymbol{n}\cdot\boldsymbol{f_1},$$

can be adopted and reads

$$v\frac{\nu_e}{2}\frac{\partial}{\partial v}\left(f_0 - 4\pi f_M\right) = v\nabla\cdot\boldsymbol{f_1} + \tilde{\boldsymbol{E}}\cdot\frac{\partial \boldsymbol{f_1}}{\partial v} + \frac{2}{v}\tilde{\boldsymbol{E}}\cdot\boldsymbol{f_1},$$
$$v\frac{\nu_e}{2}\frac{\partial \boldsymbol{f_1}}{\partial v} - \nu_{scat}\boldsymbol{f_1} = \frac{v}{3}\nabla f_0 + \frac{\tilde{\boldsymbol{E}}}{3}\frac{\partial f_0}{\partial v},$$

where $\nu_{scat} = \nu_{ei} + \frac{\nu_e}{2}$.

Kn^e	10^{-4}	10^{-3}	10^{-2}	10^{-1}	1
v_{lim}/v_{th}	70.8	22.4	7.3	3.1	1.8

TABLE II. $\sqrt{3}v\frac{\nu_e}{2} > |\tilde{\boldsymbol{E}}|$.

1. *Nonlocal electric field treatment*

$$\int_v \left(\frac{\frac{\nu_e}{2}v^2}{\nu_{scat}}\frac{\partial \boldsymbol{f_1}}{\partial v} - \frac{v^2}{3\nu_{scat}}\nabla f_0 - \frac{v}{3\nu_{scat}}\frac{\partial f_0}{\partial v}\tilde{\boldsymbol{E}} \right) v^2\,\mathrm{d}v = 0,$$

$$\left(v\frac{\nu_e}{2} - \frac{2\tilde{E}_z^2}{3v\nu_e} \right)\frac{\partial f_{1_z}}{\partial v} =$$
$$\frac{2\tilde{E}_z}{3\nu_e}\frac{\partial f_{1_z}}{\partial z} + \frac{4\pi\tilde{E}_z}{3}\frac{\partial f_M}{\partial v} + \frac{v}{3}\frac{\partial f_0}{\partial z} + \left(\frac{4\tilde{E}_z^2}{3v^2\nu_e} + \left(\nu_{ei} + \frac{\nu_e}{2}\right) \right) f_{1_z},$$

$$|\tilde{\boldsymbol{E}}_{red}| = \sqrt{3}v\frac{\nu_e}{2},$$
$$\nu_{scat}^E = \frac{|\tilde{\boldsymbol{E}}| - |\tilde{\boldsymbol{E}}_{red}|}{v},$$

where $\omega_{red} = |\tilde{\boldsymbol{E}}_{red}|/|\tilde{\boldsymbol{E}}|$.

P1 approximation equivalent

$$\tilde{f} = \frac{4\pi f_M + \delta f_0}{4\pi} + \frac{3}{4\pi}\boldsymbol{n}\cdot\boldsymbol{f_1}. \tag{13}$$

where the moment model reads

$$v\frac{\nu_e}{2}\frac{\partial \delta f_0}{\partial v} = v\nabla\cdot\boldsymbol{f_1} + \tilde{\boldsymbol{E}}\cdot\left(\omega_{red}\frac{\partial \boldsymbol{f_1}}{\partial v} + \frac{2}{v}\boldsymbol{f_1}\right),$$
$$v\frac{\nu_e}{2}\frac{\partial \boldsymbol{f_1}}{\partial v} = \tilde{\nu}_{scat}\boldsymbol{f_1} + \frac{v}{3}\nabla\left(4\pi f_M + \delta f_0\right) + \frac{\tilde{\boldsymbol{E}}}{3}\left(4\pi\frac{\partial f_M}{\partial v} + \omega_{red}\frac{\partial \delta f_0}{\partial v}\right),$$

where $\tilde{\nu}_{scat} = \nu_{ei} + \nu_{scat}^E + \frac{\nu_e}{2}$.

$$\tilde{\boldsymbol{E}} = \frac{\int_v \left(\frac{\nu_e}{2\tilde{\nu}_{scat}}v^2\frac{\partial \boldsymbol{f_1}}{\partial v} - \frac{v^2}{3\tilde{\nu}_{scat}}\nabla\left(4\pi f_M + \delta f_0\right) \right) v^2\,\mathrm{d}v}{\int_v \frac{v}{3\tilde{\nu}_{scat}}\left(4\pi\frac{\partial f_M}{\partial v} + \omega_{red}\frac{\partial \delta f_0}{\partial v}\right) v^2\,\mathrm{d}v},$$

B. Aladin, Impact, and Calder kinetic codes

C. Simulation results

V. CONCLUSIONS

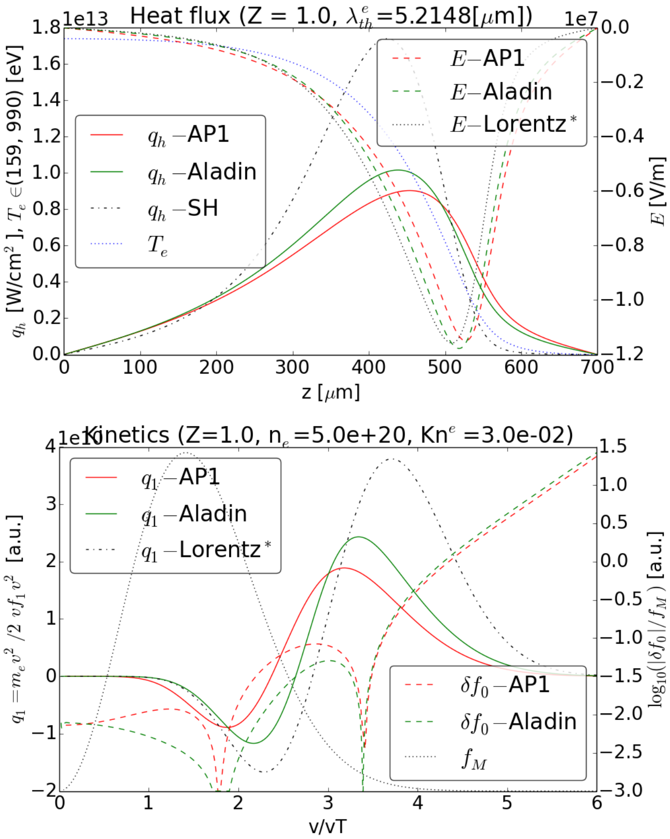

FIG. 2. Snapshot 20 ps. Left: correct steady solution of heat flux. Right: Aladins results are correct. Velocity limit 4.4 v_{th}..

[1] M. Planck, Über einen Satz der statistischen Dynamik und seine Erweiterung in der Quantentheorie, Sitzungsber. Preuss. Akad. Wiss. 24 (1917) 324–341.

[2] R. S. Cohen, L. Spitzer, Jr., P. M. Routly, The electrical conductivity of an ionized gas, Phys. Rev. 80 (1950) 230–238.

[3] L. Spitzer, Jr. and R. Härm, Transport phenomena in a completely ionized gas, Phys. Rev. 89 (1953) 977.

[4] M. N. Rosenbluth, W. M. MacDonald, D. L. Judd, Fokker-planck equation for an inverse-square force, Phys. Rev. 107 (1957) 1.

[5] J. R. Albritton, E. A. Williams, I. B. Bernstein, K. P. Swartz, Nonlocal electron heat transport by not quite maxwell-boltzmann distributions, Phys. Rev. Lett. 57 (1986) 1887–1890.

[6] N. J. Fish, Theory of current drive in plasmas, Rev. Mod. Phys. 59 (1987) 175.

[7] D. D. Sorbo, J.-L. Feugeas, P. Nicolai, M. Olazabal-Loume, B. Dubroca, S. Guisset, M. Touati, V. Tikhonchuk, Reduced entropic model for studies of multidimensional nonlocal transport in high-energy-density plasmas, Phys. Plasmas 22 (2015) 082706.

[8] D. D. Sorbo, J.-L. Feugeas, P. Nicolai, M. Olazabal-Loume, B. Dubroca, V. Tikhonchuk, Extension of a reduced entropic model of electron transport to magnetized nonlocal regimes of high-energy-density plasmas, Laser Part. Beams 34 (2016) 412–425.

[9] I. P. Shkarofsky, T. W. Johnston, M. P. Bachynskii, The particle Kinetics of Plasmas, Addison-Wesley, Reading, 1966.

[10] C. L. Longmire, Elementary Plasma Physics, Intersci. Pub., 1963.

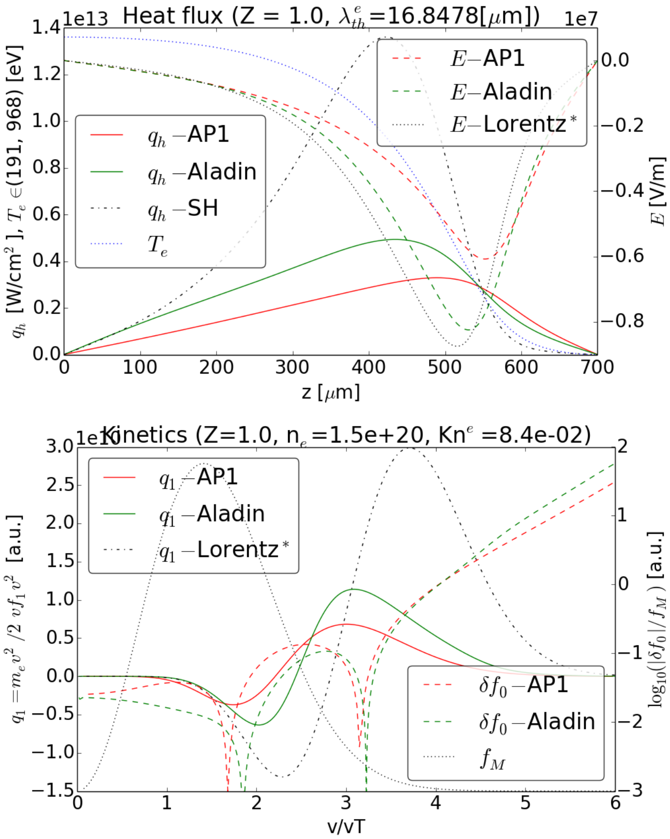

FIG. 3. Snapshot 20 ps. Left: correct steady solution of heat flux. Right: Aladins results are correct. Velocity limit 3.2 v_{th}..

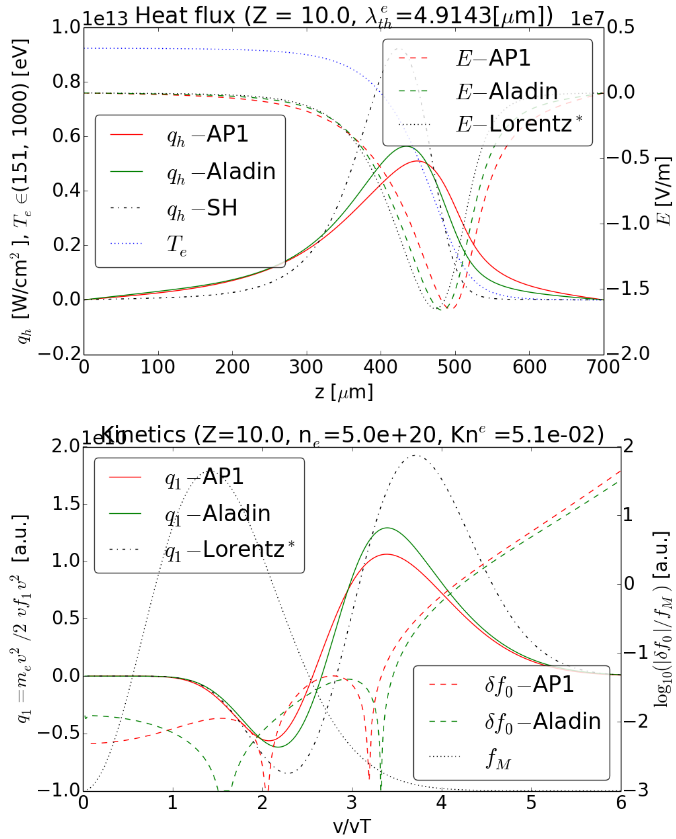

FIG. 4. Snapshot 12 ps. Left: correct steady solution of heat flux. Right: correct comparison to kinetic profiles at point 442 μm by Aladin. Velocity limit 3.4 v_{th}.

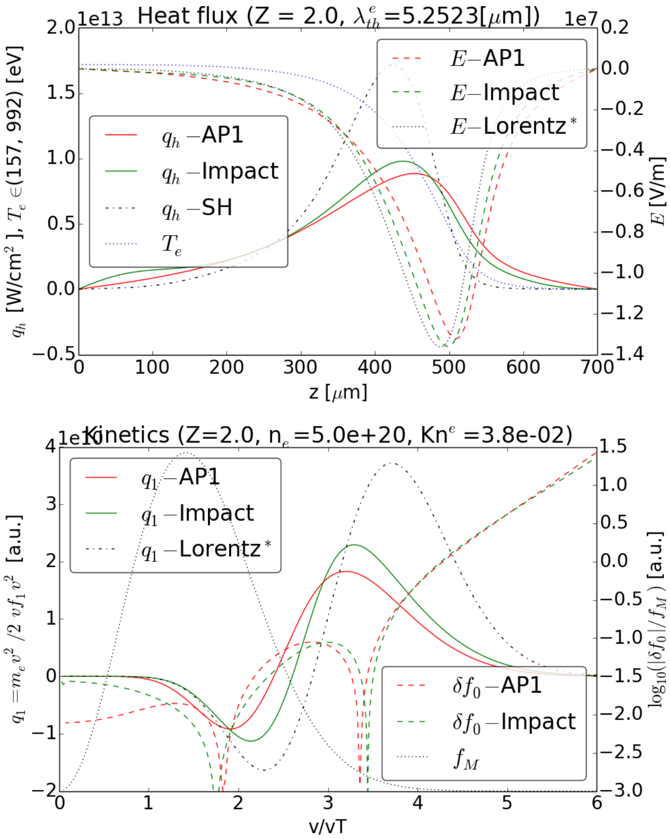

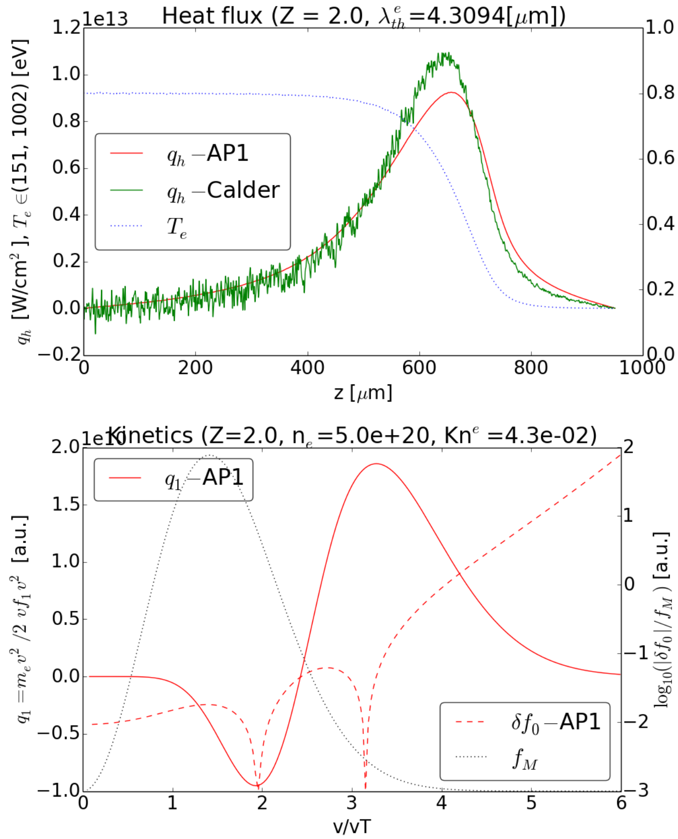

FIG. 5. Snapshot 12 ps. Left: correct steady solution of heat flux. Right: correct comparison to kinetic profiles at point 437 μm by Impact. Velocity limit 4.0 v_{th}.

FIG. 6. Snapshot 11 ps. Left: correct steady solution of heat flux. Right: Kinetic profiles at point of maximum flux by AP1. Kinetics profiles by CALDER should be added. Velocity limit 3.8 v_{th}.

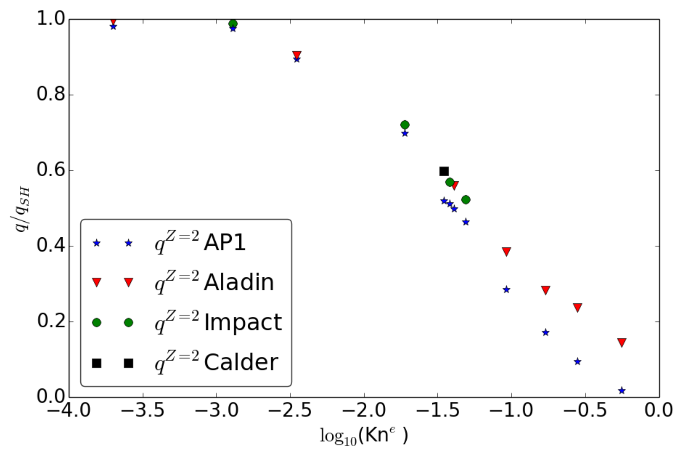

FIG. 7. Simulation results for the case $Z = 2$ computed by AP1/Aladin/Impact/Calder. Every point corresponds to the maximum heat flux in a "tanh" temperature simulation, which can be characterized by Kn. The range of $\log_{10}(\mathrm{Kn}) \in (0, -4)$ can be expressed as equivalent to the electron density approximate range $\mathrm{n}_e \in (1e19, 3.5e22)$ of the 50 μm slope tanh case. In the case of Kn $= 0.56$, $q_{Aladin}/q_{AP1} \approx 7.9$.

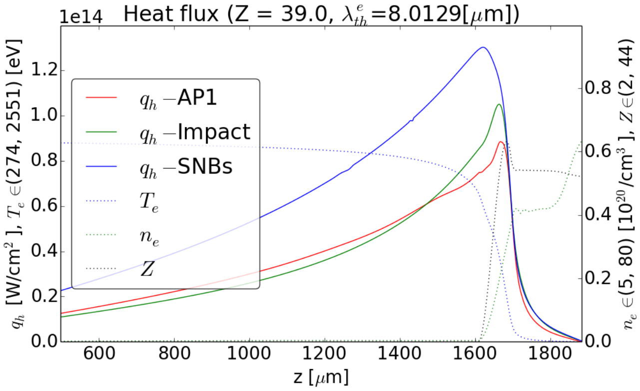

Heat flux (Z = 39.0, λ_{th}^{e}=8.0129[μm])
1e14
q_h −AP1
q_h −Impact
q_h −SNBs
T_e
n_e
Z
q_h [W/cm^2], $T_e \in$(274, 2551) [eV]
$n_e \in$(5, 80) [10^{20}/cm^3], $Z \in$(2, 44)
z [μm]

FIG. 8.